

**Supplemental Data File for:**

**mTORC1-selective activation of translation elongation promotes disease progression  
in chronic lymphocytic leukemia**

Natasha Malik<sup>1</sup>, Jodie Hay<sup>1</sup>, Hassan N.B. Almuhana<sup>1</sup>, Karen M. Dunn<sup>1</sup>, Jamie Lees<sup>1</sup>,  
Jennifer Cassels<sup>1</sup>, Jiatian Li<sup>1</sup>, Rinako Nakagawa<sup>2</sup>, Owen J. Sansom<sup>1,2</sup>, Alison M. Michie<sup>1</sup>

<sup>1</sup>Institute of Cancer Sciences, College of Medicine, Veterinary and Life Sciences,  
University of Glasgow, Glasgow UK; <sup>2</sup>Cancer Research UK Beatson Institute, Gartnavel  
Estate, Glasgow, UK. <sup>3</sup>Cancer Research UK Beatson Institute; Gartnavel Estate, Glasgow,  
UK.

## Supplementary Methods:

*Cell Culture conditions:* Primary CLL cells and the MEC1 CLL cell line were cultured at  $1 \times 10^6$ /mL in RPMI-1640 containing 10% foetal bovine serum (FBS), 50 U/mL penicillin, 50 mg/mL streptomycin, and 2 mM L-glutamine (CLL medium; Invitrogen Ltd., Paisley, UK). OP9 stromal cells were maintained in OP9 medium ( $\alpha$ MEM medium supplemented with 20% FBS, 50 U/mL penicillin, 50 mg/mL streptomycin, 2 mM L-glutamine, 10 mM HEPES, 1 mM sodium pyruvate, 10  $\mu$ g/ml gentamycin, 50  $\mu$ M  $\beta$ ME). The fibroblast cell line constitutively expressing CD40L (NTL-CD40L) was maintained in CLL medium. All cells were cultured at 37°C in a humidified incubator with 5% (v/v) CO<sub>2</sub>. Cell lines were authenticated based on functional capacity, morphology and/or phenotype, and were tested for the mycoplasma contamination once every 6-8 months.

*In vitro OP9 co-culture of retrovirally-transduced HPCs:* LSKs were retrovirally-transduced with either empty vector (MIEV) or kinase dead PKC $\alpha$  (PKC $\alpha$ -KR) vector to induce a CLL-like disease.<sup>1</sup> Cells were co-cultured with the OP9 cell line supplemented with IL-7 and Flt-3 (each 10 ng/mL) until day 7-10, passaging every 2-3 days. After d10, cells were further co-cultured with OP9 and IL-7 only. To induce *Raptor*-excision *in vitro*, retrovirally-transduced HPCs from *Mx1-Raptor* mice were co-cultured with OP9 cells *in vitro* until d10. Then  $0.5-1 \times 10^6$  cells/well were treated with 200 U/well IFN $\beta$  for 24 hr to excise *Raptor*. The cells were harvested 4 days post treatment and used in ongoing experiments, as indicated.

*Migration Assay:* CD19-*Raptor*-PKC $\alpha$ -KR cells ( $2-5 \times 10^6$  cells/ml) were cultured for 2 hr at 37°C in resting medium (DMEM containing 0.5% bovine serum albumin (BSA), 10 mM HEPES, 1 mM sodium pyruvate, 100  $\mu$ g/ml streptomycin, 100 U/ml penicillin, 2 mM L-glutamine). Resting medium was supplemented with 150 ng/ml SDF-1 (PeproTech, UK) to make migration medium. Transwell<sup>®</sup> permeable support chambers (6.5 mm-diameter upper chamber, pore diameter 5  $\mu$ m transwell culture insert; Corning Inc, ME, USA) were set up such that the bottom contained 600  $\mu$ l migration medium and 100  $\mu$ l cells from the resting step was pipetted onto the top chamber. Each condition was carried out in technical duplicates. For negative and positive controls, resting medium was used instead of the migration medium: rested cells were either pipetted onto the chamber or directly into the bottom respectively. Cells were cultured at 37°C for 4 hr. 150  $\mu$ l medium was pipetted from every well in technical triplicate and counted on the flow cytometer on low for 30 sec. Data shown is an average of 3 individual mice.

*Primary CLL proliferation co-cultures:* CLL cells were co-cultured with the NTL-CD40L cell line at a ratio of 1:75, as described previously.<sup>2,3</sup> The culture was supplemented with 15 ng/mL IL-21 (PeproTech, UK) to induce proliferation for 5-8 days. These co-cultures were treated with DMSO

as vehicle/no drug control (NDC), 10 nM rapamycin (RAP), 100 nM AZD8055 (AZD or A8055), 1  $\mu$ M ibrutinib (IB), 500 nM AZD2014 (A2014) or RAP/IB or AZD/IB combinations, as indicated.

**Flow Cytometry:** Single cell suspensions from *in vivo* or *in vitro* experiments were prepared for phenotypic analysis by flow cytometry as described previously.<sup>4,5</sup> All antibodies were purchased from BD Biosciences (Oxford, UK), except CD21 (Clone: 7E9, BioLegend), CD1d (Clone: 1B1, BioLegend), IgD (Clone: 11-26c.2a, BioLegend), CD23 (Clone: B3B4, BioLegend). For cell cycle analysis, treated  $1 \times 10^6$  PKC $\alpha$ -KR and  $2 \times 10^6$  primary CLL patient cells were fixed and permeabilized by adding 1 ml cold 80% ethanol dropwise to the pellet and stored at  $-20^\circ\text{C}$  until analysis. After washing the samples, 350-500  $\mu$ l propidium iodide (PI)/RNase Staining Buffer (BD Biosciences) was added to each sample and incubated at RT in the dark for 15 min before analysis. For cell proliferation, cells were stained with CellTrace™ Violet stock solution (Invitrogen, Paisley, UK) as per the manufacturer's protocol. PKC $\alpha$ -KR cells were acquired for 3 consecutive days (every 24 hr) and primary CLL patient samples were recorded on day 5-8 of culture to assess proliferation. For apoptosis analysis, treated  $5 \times 10^5$  PKC $\alpha$ -KR or primary CLL patient cells were washed with 1x HBSS (ThermoFisher Scientific) at 300g for 5 min at RT. Cells were incubated in 100  $\mu$ l HBSS containing 2.5  $\mu$ l Annexin V and 2.5  $\mu$ l 7AAD (BD Biosciences) for 10 min at RT in the dark and analysed. Data were acquired on a FACSCantoII with BD FACSDiva software and analysed using FlowJo software (Tree Star Inc., OR).

**qPCR:** RNA was extracted from fresh cells following the RNeasy Qiagen Kit protocol. cDNA was made using standard protocols (Invitrogen). qPCR was carried out on a 384 well plate in triplicate by the 7900HT Fast Real-Time PCR system (Applied Biosystems, Warrington, UK). The primers used are listed in Table S2. *Raptor* excision PCR: Successful recombination by Cre recombinase (using *Rptor* for and *Rptor* del primers) resulted in a 204bp product (del).<sup>6</sup> In brief, 240 ng/25  $\mu$ l of DNA was amplified in a PCR reaction with a hot start of  $95^\circ\text{C}$  for 2 min followed by 40 cycles of: 30 sec denaturation at  $95^\circ\text{C}$ , 30 sec annealing at  $59^\circ\text{C}$ , 1 min extension at  $72^\circ\text{C}$ ; and a final extension at  $72^\circ\text{C}$  for 5 min, before separating with gel electrophoresis.

**Western blotting:** Protein lysates of cell pellets were prepared in lysis buffer (20 mM Tris pH 7.4, 2mM EDTA, 1% Triton, 1mM DTT) containing protease inhibitor cocktail and phosphatase inhibitor cocktail (Roche) and incubated on ice for 30 min. Bradford assay was performed to quantify protein samples using a standard protocol (Bio-Rad). 4-12% pre-cast gels (NuPAGE Novex BisTris) were used for gel electrophoresis. Western blotting was performed by following the standard protocol provided (Invitrogen). The PVDF membranes were blocked in 5% milk and primary antibodies used were prepared in 1% BSA. List of antibodies are listed in Table S3. Signals were detected using Imobilon Forte HRP substrate (Millipore).

*Protein Synthesis Assay:* The O-Propargyl-puromycin (OPP) incorporation was performed as part of the Global Protein Synthesis Assay (Abcam), as per manufacturer's instructions. In brief, following drug treatments,  $1 \times 10^5$  cells/100  $\mu$ L were transferred to a 96 well plate. A control well was incubated with 1X cycloheximide for 1 hr. All samples were the incubated with 1X Protein label for 1 hr before fixing and permeabilising the cells and then staining with the reaction protocol as outlined in the protocol. Samples were analysed by flow cytometry for the amount of fluorescence generated by *de novo* synthesized protein during the Click reaction

*MEC1 Transient Transfection:* Raptor knockdown in MEC1 cells was performed by delivery of an shRNA construct targeting Raptor (MISSION® shRNA, Sigma Aldrich) with Lipofectamine 2000 reagent (Thermo Fisher Scientific). In brief, DNA-lipid complex was prepared with plasmid DNA targeting Raptor or scrambled control in a 1:5 ratio (1  $\mu$ g DNA: 5  $\mu$ l transfection reagent) to  $1 \times 10^6$  MEC1 cells in a 48 well plate. Cells were incubated for 3 days prior to experimental set up.

## References

1. Nakagawa R, Soh JW, Michie AM. Subversion of Protein Kinase C $\alpha$  Signaling in Hematopoietic Progenitor Cells Results in the Generation of a B-Cell Chronic Lymphocytic Leukemia–Like Population In vivo. *Cancer Res.* 2006;66(1):527–34.
2. McCaig AM, Cosimo E, Leach M, Michie AM. Dasatinib inhibits CXCR4 signaling in chronic lymphocytic leukemia cells and impairs migration towards CXCL12. *PLoS One.* 2012;7:e48929.
3. Pascutti MF, Jak M, Tromp JM, Derks IAM, Remmerswaal EBM, Thijssen R, et al. IL-21 and CD40L signals from autologous T cells can induce antigen-independent proliferation of CLL cells. *Blood.* 2013;122:3010-9.
4. Malik N, Dunn K, Cassels J, Hay J, Estell C, Sansom OJ, et al. mTORC1 activity is essential for erythropoiesis and B cell lineage commitment. *Sci Rep.* 2019;9:16917.
5. Cosimo E, Tarafdar A, Moles MW, Holroyd AK, Malik N, Catherwood MA, et al. AKT/mTORC2 Inhibition Activates FOXO1 Function in CLL Cells Reducing B-Cell Receptor-Mediated Survival. *Clin Cancer Res.* 2019 Mar;25(5):1574–87.
6. Bentzinger CF, Romanino K, Cloëtta D, Lin S, Mascarenhas JB, Oliveri F, et al. Skeletal Muscle-Specific Ablation of raptor, but Not of rictor, Causes Metabolic Changes and Results in Muscle Dystrophy. *Cell Metab.* 2008;8(5):411–24.

CLL ID	Treatment <sup>a</sup>	Sex	Binet Stage	ZAP-70 status <sup>b</sup>	Cytogenetics
9	No	F	A	neg	No 11q/17p
113	Yes	F	C	high	del17p
116	No	M	A	high	No 11q/17p
140	No	F	A	low	T12
147	No	M	C	high	No 11q/17p
151	No	M	B	ND	del11q
165	No	M	C	ND	del11q
168	Yes	M	B	ND	del13q, T12
169	No	F	C	ND	del11q
171	No	M	C	ND	No 11q/17p
173	Yes	M	B	ND	del11q
175	Yes	M	C	ND	No 11q/17p
176	No	M	A	ND	No 11q/17p
177	No	M	B	ND	No 11q/17p
179	Yes	M	B	ND	No 11q/17p
180	Yes	F	B	ND	No 11q/17p
185	Yes	M	C	ND	ND
186	No	M	C	ND	ND
187	No	M	B	ND	ND
189	Yes	M	B	ND	No 11q/17p
190	No	M	C	ND	No 11q/17p
191	No	M	A	ND	del11q, del17p
193	No	F	A	ND	No 11q/17p
194	No	M	C	ND	ND

**Table S1. CLL patient clinical characteristics.**

<sup>a</sup> If previously undergone treatment, it was not within three months of sample collection.

<sup>b</sup> ZAP-70 analysis was conducted by immunohistochemistry in the regional haematology laboratory. ND – not determined.

<b>Gene</b>	<b>Forward</b>	<b>Reverse</b>	<b>Species</b>	<b>Sequence Information</b>
<b><i>Ebf1</i></b>	tacagaaggctcattcctcgg	atcccatacagggcttcaac	Mouse	NM_001290709.1
<b><i>Pax5</i></b>	acagga catggaggag tga	tgacaccttg atgggcaagt	Mouse	NM_008782.2
<b><i>Rptor</i></b>	atggtagcaggcacactctcatg	gctaaacattcagtcctaatac	Mouse	Ref. 5
<b><i>Rptor-del</i></b>	ctcagagaactgcagtgctgaagg		Mouse	Ref. 5
<b><i>Gusb</i></b>	taagacgctgatcaccaca	cagataaacatccacgtacgg	Mouse	NM_010368.1
<b><i>Tbp</i></b>	gtacccttcaccaatgactc	cagccaagattcacggtaga	Mouse	NM_013684.3

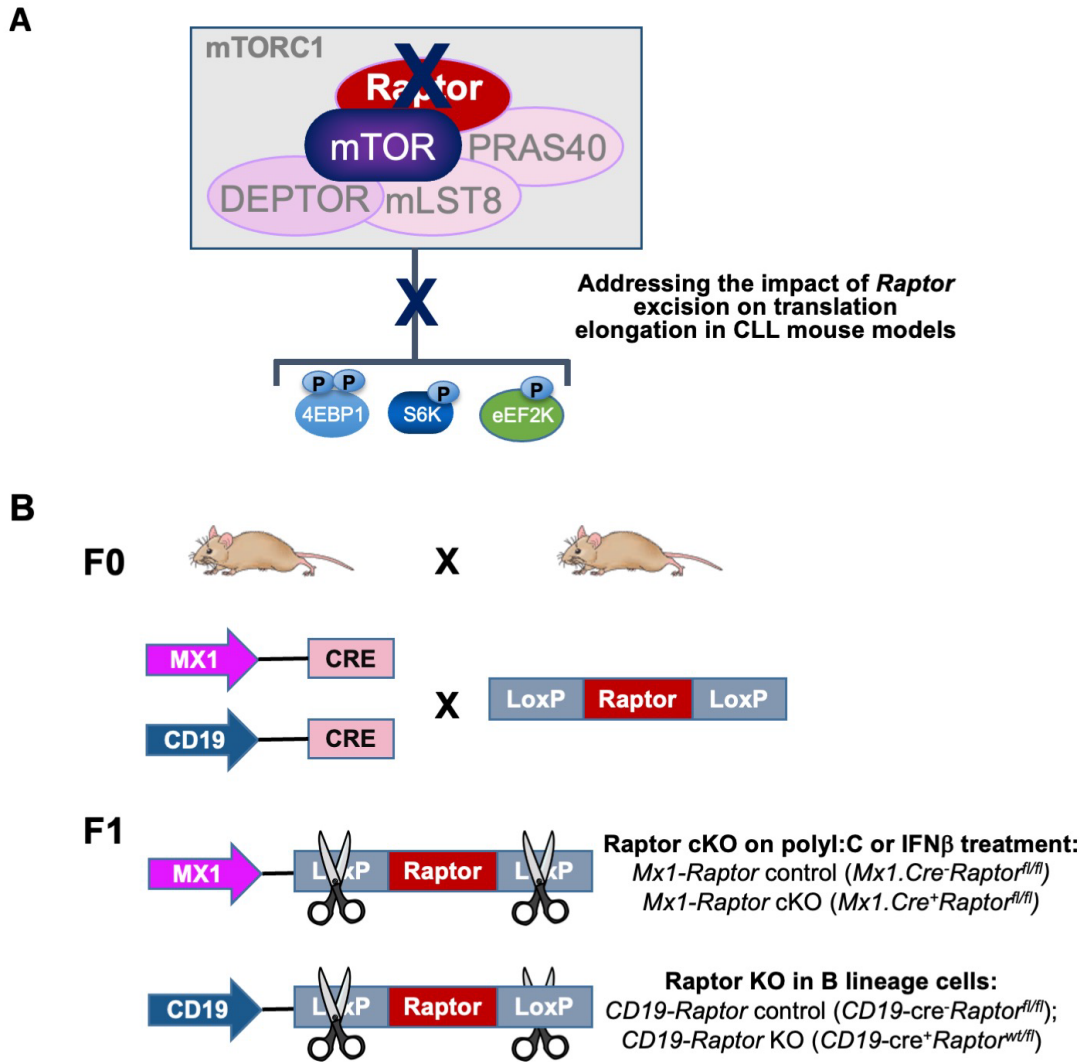
**Table S2: List of primers used for PCR reactions.**

The full sequence for each gene was obtained from the NCBI gene database (<https://ncbi.nlm.nih.gov/gene>). Each primer was designed to have close to 10 C=G and 10 A=T bonds. The length between the forward and reverse primer is between 150-300 base pairs. *Gusb* and *Tbp* were used as reference genes for murine cells. The specificity of each primer sequence was checked by using BLASTn tool.

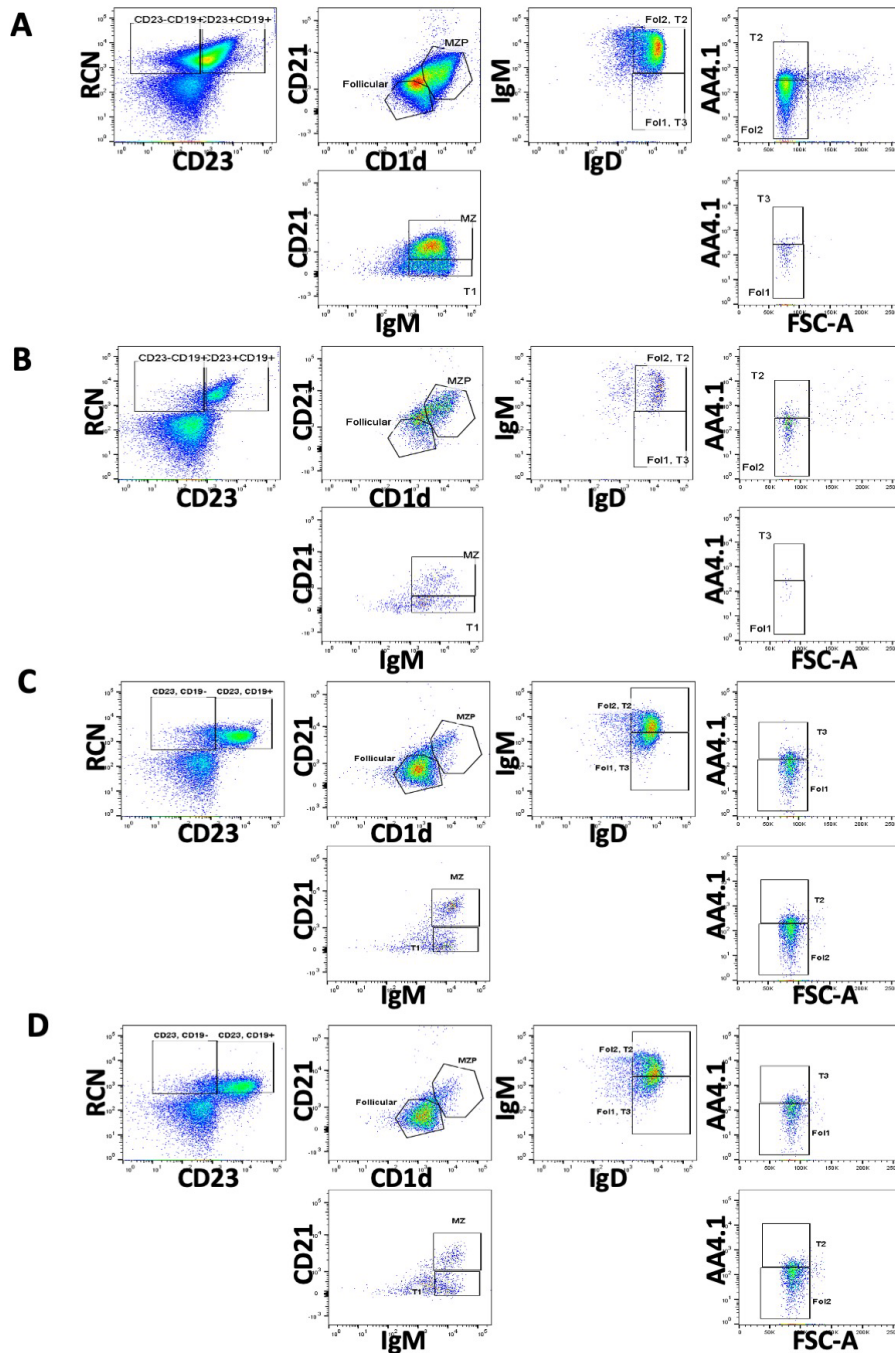
<b>Name</b>	<b>Named Species Reactivity</b>	<b>Clone</b>	<b>Dilution</b>	<b>2<sup>nd</sup>ary Ab</b>
<b>RAPTOR</b>	Human, Mouse, Rat	24C12	1:1000	Rabbit
<b>pAKT<sup>S473</sup></b>	Human, Mouse, Rat	D9E	1:1000	Rabbit
<b>AKT (pan)</b>	Human, Mouse, Rat	C67E7	1:1000	Rabbit
<b>pS6<sup>S235/S236</sup></b>	Human, Mouse, Rat	D57.2.2E	1:1000	Rabbit
<b>S6</b>	Human, Mouse, Rat	54D2	1:1000	Mouse
<b>p4EBP1<sup>T37/T46</sup></b>	Human, Mouse, Rat	236B4	1:1000	Rabbit
<b>peEF2<sup>T56</sup></b>	Human, Mouse, Rat	#2331	1:1000	Rabbit
<b>eEF2</b>	Human, Mouse, Rat	#2332	1:1000	Rabbit
<b>peEF2k<sup>S366</sup></b>	Human, Rat, Monkey	#3691	1:500	Rabbit
<b>eEF2k</b>	Human, Rat, Monkey	#3692	1:500	Rabbit
<b>Cyclin A</b>	Human, Mouse	C-19	1:1000	Rabbit
<b>Mcl1</b>	Human, Mouse	D34A5	1:1000	Rabbit
<b>4EBP1</b>	Human, Mouse, Rat	53H11	1:1000	Rabbit
<b>GAPDH</b>	Human, Mouse, Rat	D16H11	1:1000	Rabbit
<b><math>\beta</math>-ACTIN</b>	Human, Mouse, Rat	C4	1:1000	Mouse
<b><math>\alpha</math>-mouse IgG, HRP Ab</b>			1:10000	
<b><math>\alpha</math>-rabbit IgG, HRP Ab</b>			1:10000	

**Table S3: List of antibodies used for western blotting.**

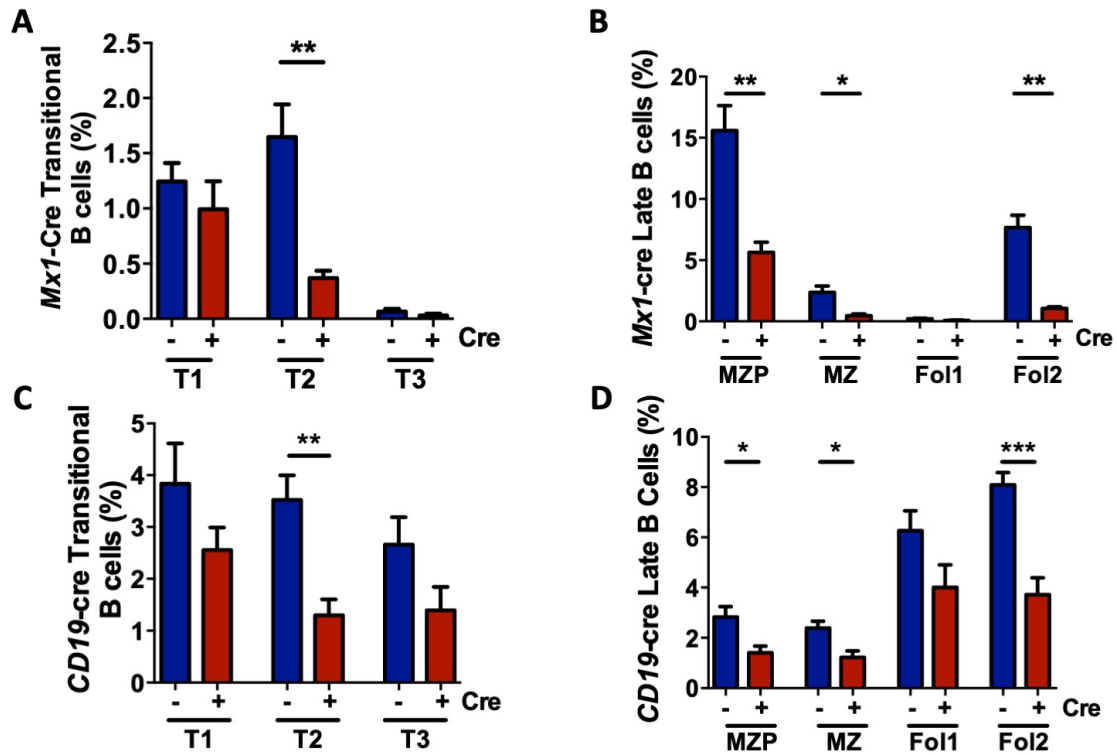
List of antibodies (Ab) and their dilutions in 5% BSA in TBS-T. All antibodies were purchased from Cell Signalling Technologies (Herts, UK), except Cyclin A and  $\beta$ -Actin (Santa Cruz, USA).



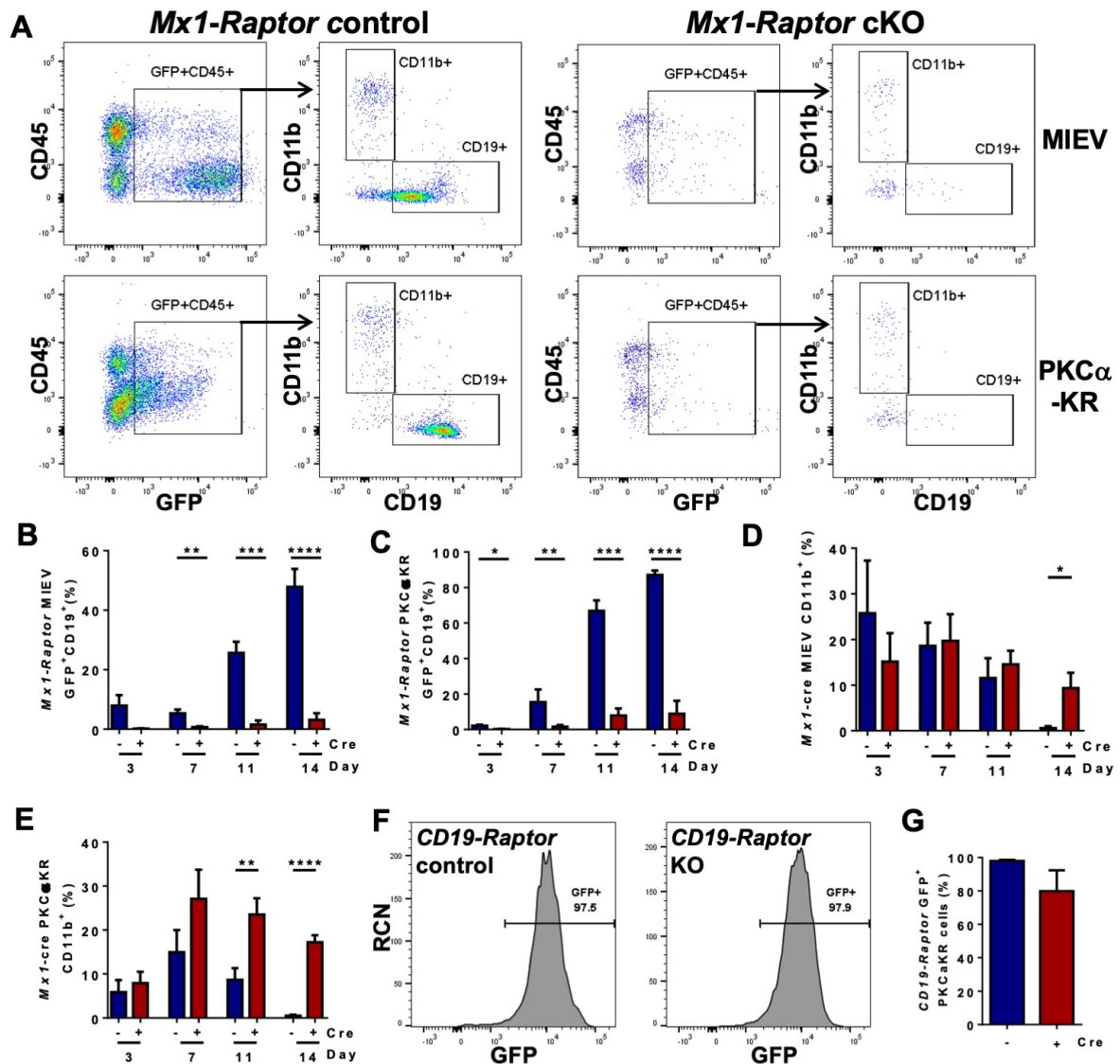
**Supplementary Figure 1: Diagrammatic representation of the mouse models used in this study.** (A) A simplified signalling diagram showing the impact of *Raptor* excision from mice on downstream mTORC1 signalling, resulting in a blockage of mTORC1-mediated phosphorylation of key downstream mediators of protein translation. (B) Generation of *Raptor* knockout (KO) mouse models *in vivo*: *Mx1-Raptor* conditional KO (cKO) mice, where excision of *Raptor* is induced post 4 polyI:C inoculations *in vivo*. This was performed in Cre- (*Mx1-Raptor* control) and Cre+ (*Mx1-Raptor* cKO) mice. Expressing *Cre* under the CD19-promotor resulted in the excision of *Raptor* in B lineage cells only: *CD19-Raptor* control (*CD19-cre-Raptor<sup>fl/fl</sup>*) and *CD19-Raptor* KO (*CD19-cre<sup>+</sup>Raptor<sup>wt/fl</sup>*).



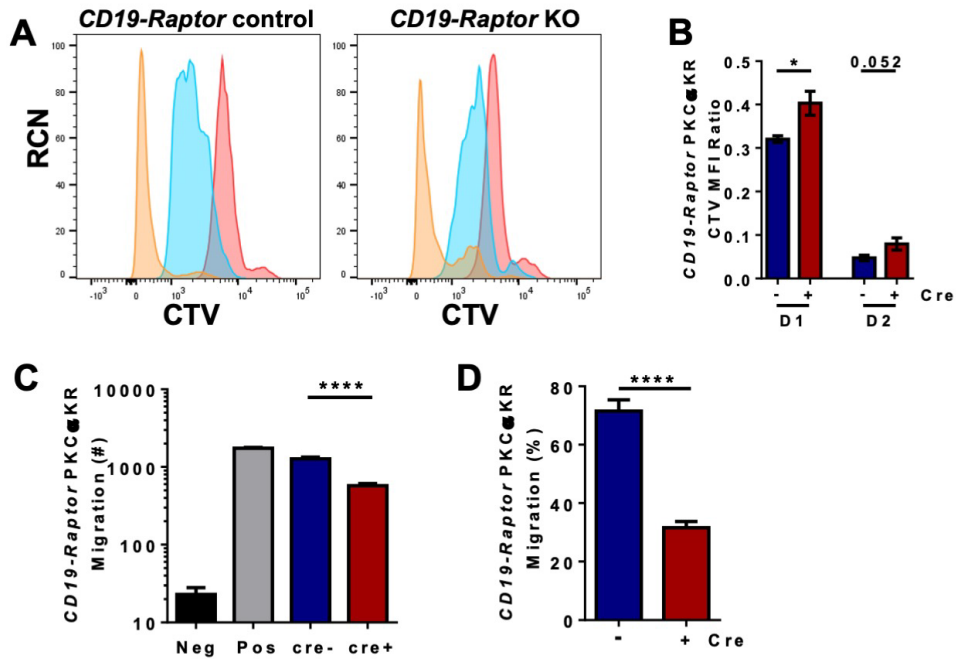
**Supplementary Figure 2: Raptor-deficiency in adult mice leads to aberrations in late B cells *in vivo*.** Representative flow cytometry plots demonstrating the gating strategy and the proportion of late B cells which comprise transitional 1 (T1) cells (CD19<sup>+</sup>CD21<sup>int</sup>CD23<sup>-</sup>IgM<sup>high</sup>); T2 (CD19<sup>+</sup>AA4.1<sup>+</sup>CD21<sup>int</sup>CD23<sup>+</sup>CD1d<sup>int</sup>IgD<sup>high</sup>IgM<sup>high</sup>); T3 (CD19<sup>+</sup>AA4.1<sup>+</sup>CD21<sup>int</sup>CD23<sup>+</sup>CD1d<sup>int</sup>IgD<sup>high</sup>IgM<sup>low</sup>); marginal zone precursor (MZP): (CD19<sup>+</sup>CD21<sup>high</sup>CD23<sup>+</sup>CD1d<sup>high</sup>); marginal zone (MZ) (CD19<sup>+</sup>CD21<sup>high</sup>CD23<sup>-</sup>CD1d<sup>high</sup>); Fo1 (CD19<sup>+</sup>AA4.1<sup>-</sup>CD21<sup>low</sup>CD23<sup>+</sup>CD1d<sup>int</sup>IgD<sup>high</sup>IgM<sup>low</sup>) Fo2 (CD19<sup>+</sup>AA4.1<sup>-</sup>CD21<sup>low</sup>CD23<sup>+</sup>CD1d<sup>int</sup>IgD<sup>high</sup>IgM<sup>high</sup>) in the spleen in *Mx1-Raptor* control (A), *Mx1-Raptor* cKO mice assessed 5 wks post 4 polyI:C inoculations (B), CD19-Raptor control (*CD19-cre<sup>+</sup>Raptor<sup>fl/fl</sup>*) (C) and CD19-Raptor KO (*CD19-cre<sup>+</sup>Raptor<sup>wt/fl</sup>*) (D) mice.



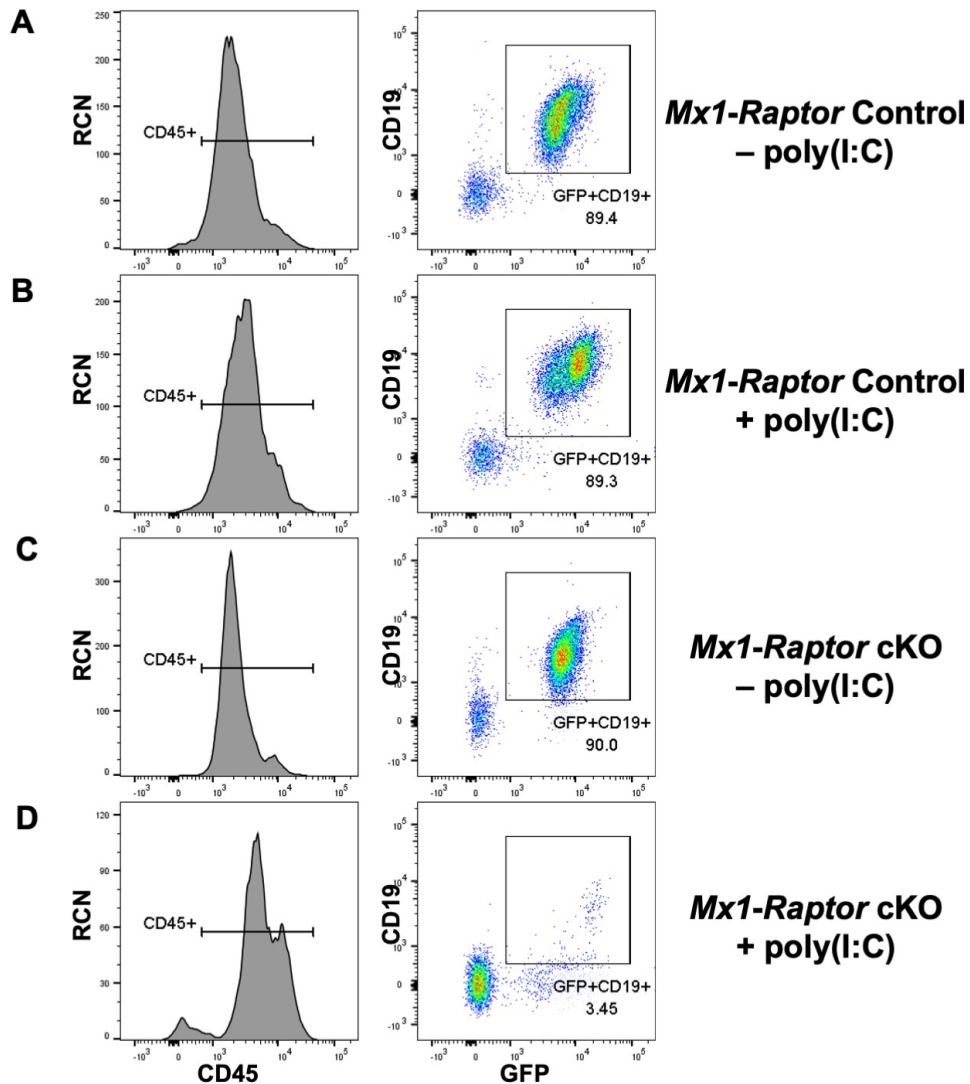
**Supplementary Figure 3: *Raptor*-deficiency in adult mice leads to aberrations in late B cells *in vivo*.** Bar graphs demonstrating the percentage of T1, T2 and T3 B cells (A), along with the percentage of MZP, MZ, Fol1, and Fol2 cells (B) in the spleen in *Mx1-Raptor* control and *Mx1-Raptor* cKO mice 5 wks post 4 poly:I:C inoculations. Bar graphs demonstrating the percentage of T1, T2 and T3 B cells (C), along with the percentage of MZP, MZ, Fol1, and Fol2 cells (D) in the spleen in *CD19-Raptor* control and *CD19-Raptor* KO mice. Data are expressed as mean  $\pm$  SEM. p values were determined by two-tailed unpaired *t*-test (p  $\leq$  0.05, p  $\leq$  0.001).



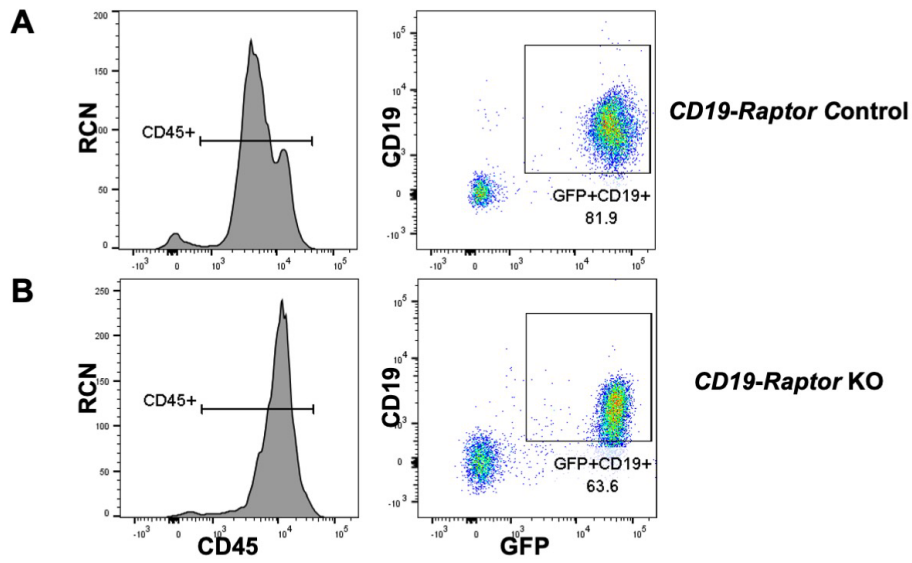
**Supplementary Figure 4: Raptor-deficiency in *Mx1-cre* mice blocks the development of CLL-like disease from HPCs *in vitro*.** **A.** BM-derived HPCs were isolated from poly(I:C)-treated mice 5 wk post 4 poly(I:C) inoculation. Representative flow cytometry plots show D7 co-cultures post retroviral transduction with either GFP-tagged MIEV construct into BM-derived HPCs from *Mx1-Raptor* control (left, top) or cKO (right, top) mice, or GFP-tagged PKC $\alpha$ -KR construct into BM-derived HPCs from *Mx1-Raptor* control (left, bottom) or cKO (right, bottom). Plots were live and size (FSC/SSC) gated, and doublet cells were excluded and were gated for GFP<sup>+</sup>CD45<sup>+</sup> before assessing surface expression of CD19<sup>+</sup> or CD11b<sup>+</sup> populations. Percentage of CD19<sup>+</sup>GFP<sup>+</sup> population of *Mx1-Raptor* control or cKO MIEV (**B**) and *Mx1-Raptor* control or cKO PKC $\alpha$ -KR (**C**) cells over D3 (n=3), D7 (n=6), D11 (n=6), and D14 (n=6) of culture, together with percentage of CD11b<sup>+</sup> population of *Mx1-Raptor* control or cKO MIEV (**D**) and *Mx1-Raptor* control or cKO PKC $\alpha$ -KR (**E**) cells over D3 (n=5), D7 (n=9), D11 (n=8) and D14 (n=8) of culture. **F.** Representative flow cytometry plots showing D17 post the retroviral transduction of GFP-tagged PKC $\alpha$ -KR construct into purified CD11b<sup>+</sup> lymphocytes from the BM of *CD19-Raptor* control (left) or KO (right) mice. Plots were live and size (FSC/SSC-A) gated, and doublet cells were excluded and were gated for GFP<sup>+</sup> cells. **G.** Percentage of GFP<sup>+</sup> PKC $\alpha$ -KR cells transduced from *CD19-Raptor* control BM (blue) or *CD19-Raptor* KO mice (red). Data are expressed as mean  $\pm$  SEM. p values were determined by two-tailed unpaired *t*-test (p \* $\leq$  0.05, p \*\* $\leq$  0.001, p \*\*\* $\leq$  0.0001, p \*\*\*\* $\leq$  0.00001).



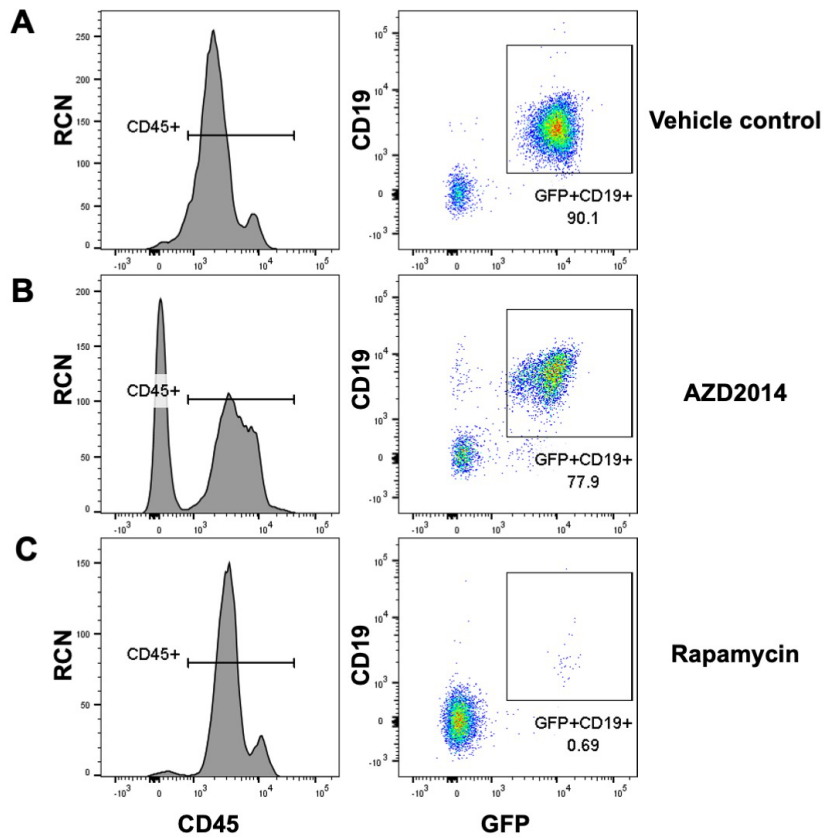
**Supplementary Figure 5: *Raptor*-deficiency in CD19<sup>+</sup> CLL-like cells leads to decreased cellular proliferation and migration *in vitro*.** **A.** Representative plot showing CTV proliferation assay performed every 24 hr for 72 hr (red = 24 hr; blue = 48 hr; orange = 72 hr) on *CD19-Raptor* control (left) or KO (right) PKC $\alpha$ -KR cells at d18 of co-culture. Bar graphs demonstrating CTV MFI ratios of D1/D0 and D2/D0 of *CD19-Raptor* control (n=5) and *CD19-Raptor* KO PKC $\alpha$ -KR cells (n=3) (**B**). Cell number (**C**) and percentage (**D**) of migration of *CD19-Raptor* control (n=3) and *CD19-Raptor* KO (n=3) PKC $\alpha$ -KR cells towards SDF-1 after serum starvation. Negative and positive controls represent migration without SDF-1 and 100% migration respectively. Data are expressed as mean  $\pm$  SEM. p values were determined by two-tailed unpaired *t*-test (p  $\leq$  0.05, p  $\leq$  0.001, p  $\leq$  0.0001, p  $\leq$  0.00001).



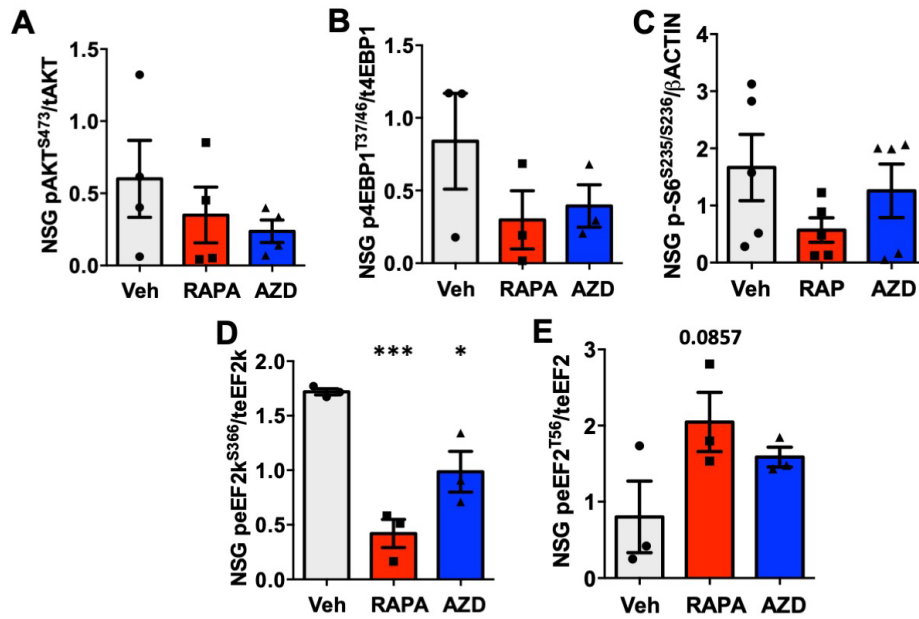
**Supplementary Figure 6: Induced *Raptor*-deficiency after disease development abrogates CLL-like disease *in vivo*.** NSG host mice were transplanted with *Mx1-Raptor* PKC $\alpha$ KR cells and allowed to develop a CLL-like disease. Representative flow cytometry plots showing proportion of GFP<sup>+</sup>CD45<sup>+</sup>CD19<sup>+</sup> CLL-like PKC $\alpha$ -KR cells in a blood sample taken from NSG mice which were transplanted with 5x10<sup>5</sup> *Mx1-Raptor* control PKC $\alpha$ -KR cells (**A**), *Mx1-Raptor* control PKC $\alpha$ -KR cells and given 4 inoculation of poly(I:C) after disease development (**B**), *Mx1-Raptor* cKO PKC $\alpha$ -KR cells (**C**) and *Mx1-Raptor* cKO-PKC $\alpha$ -KR cells and given 4 inoculation of poly(I:C) after disease development (**D**). Plots are live and size (FSC/SSC) gated prior to the gating shown. Doublet cells were excluded (FSC-A/FSC-H) and positively selected for CD45 before assessing surface expression of GFP<sup>+</sup>CD19<sup>+</sup> population. Relative Cell Number (RCN).



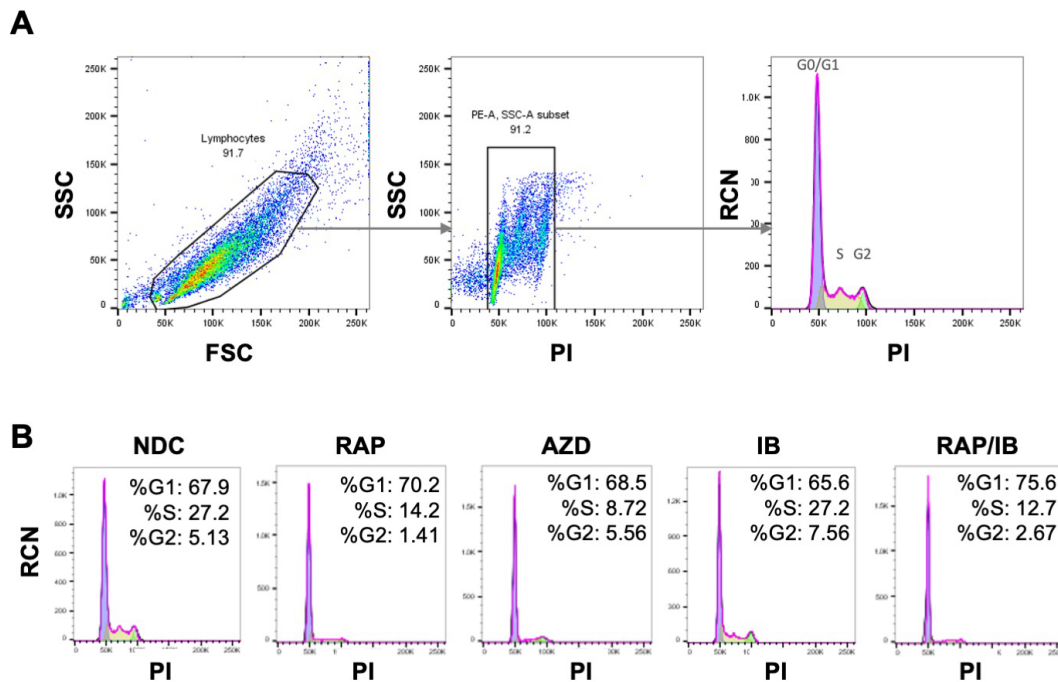
**Supplementary Figure 7: Raptor-deficiency in CD19<sup>+</sup> CLL-like cells does not block CLL-like disease accumulation *in vivo*.** NSG mice were transplanted with *CD19-Raptor* PKC $\alpha$ -KR cells and CLL-like disease was established. Representative flow cytometry plots showing proportion of GFP<sup>+</sup>CD45<sup>+</sup>CD19<sup>+</sup> CLL-like PKC $\alpha$ -KR cells in the blood of NSG mice transplanted with *CD19-Raptor* control (**A**) or *CD19-Raptor* KO (**B**) PKC $\alpha$ -KR cells. Plots are live and size (FSC/SSC) gated prior to the gating shown. Doublet cells were excluded (FSC-A/FSC-H) and positively selected for CD45 before assessing surface expression of GFP<sup>+</sup>CD19<sup>+</sup> population.



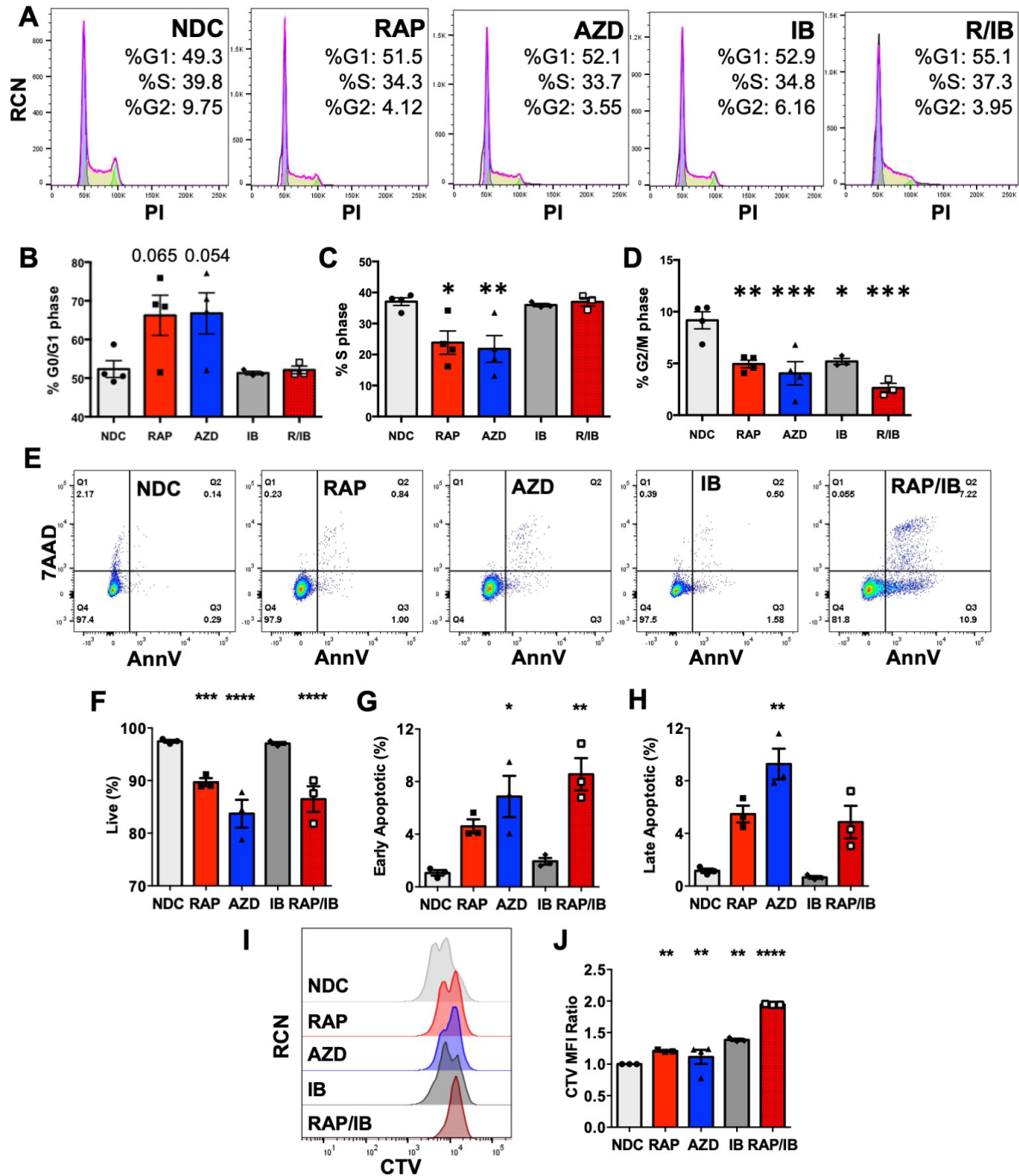
**Supplementary Figure 8: Secondary transplanted mice with an aggressive CLL-like disease have the greatest decrease in disease load with rapamycin treatment *in vivo*.** NSG host mice were transplanted with PKC $\alpha$ -KR cells from the spleen of NSG mice with  $\geq 95\%$  CLL-like disease. Representative flow cytometry plots showing proportion of GFP<sup>+</sup>CD45<sup>+</sup>CD19<sup>+</sup> CLL-like PKC $\alpha$ -KR cells in the blood of NSG mice which were treated with either vehicle control (captisol) (A), AZD2014 (B), rapamycin (C). Plots are live and size (FSC/SSC) gated prior to the gating shown. Doublet cells were excluded (FSC-A/FSC-H) and positively selected for CD45 before assessing surface expression of GFP<sup>+</sup>CD19<sup>+</sup> population.



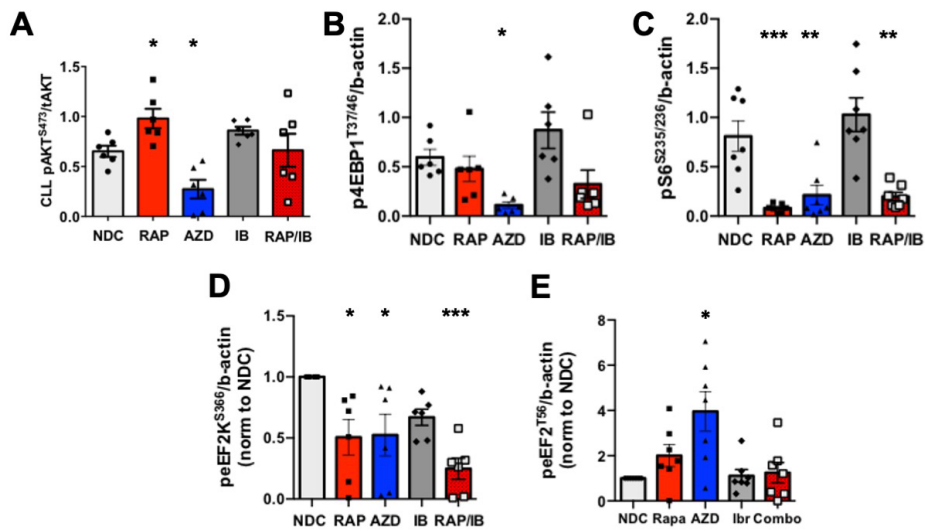
**Supplementary Figure 9: A potentially different mechanism of rapamycin reducing an aggressive CLL-like disease load compared to AZD2014 *in vivo*.** Protein lysates were prepared from spleen of secondary transplants of PKC $\alpha$ -KR cells after drug treatment. Densitometry plots of western blots including Figure 5H. Graphs show pAKT<sup>S473</sup>/AKT, p4EBP1<sup>T37/46</sup>/4EBP1, pS6<sup>S235/S236</sup>/ $\beta$ -Actin, peEF2<sup>T56</sup>/eEF2 and peEF2<sup>K</sup><sup>S366</sup>/eEF2K of the spleens of mice with disease and treated with either Veh (n $\geq$ 3), RAP (n $\geq$ 3) or AZD (n $\geq$ 3). Data are expressed as mean  $\pm$  SEM. p values were determined by an ordinary one-way ANOVA with Dunnett multiple comparisons test (p  $\leq$ 0.05).



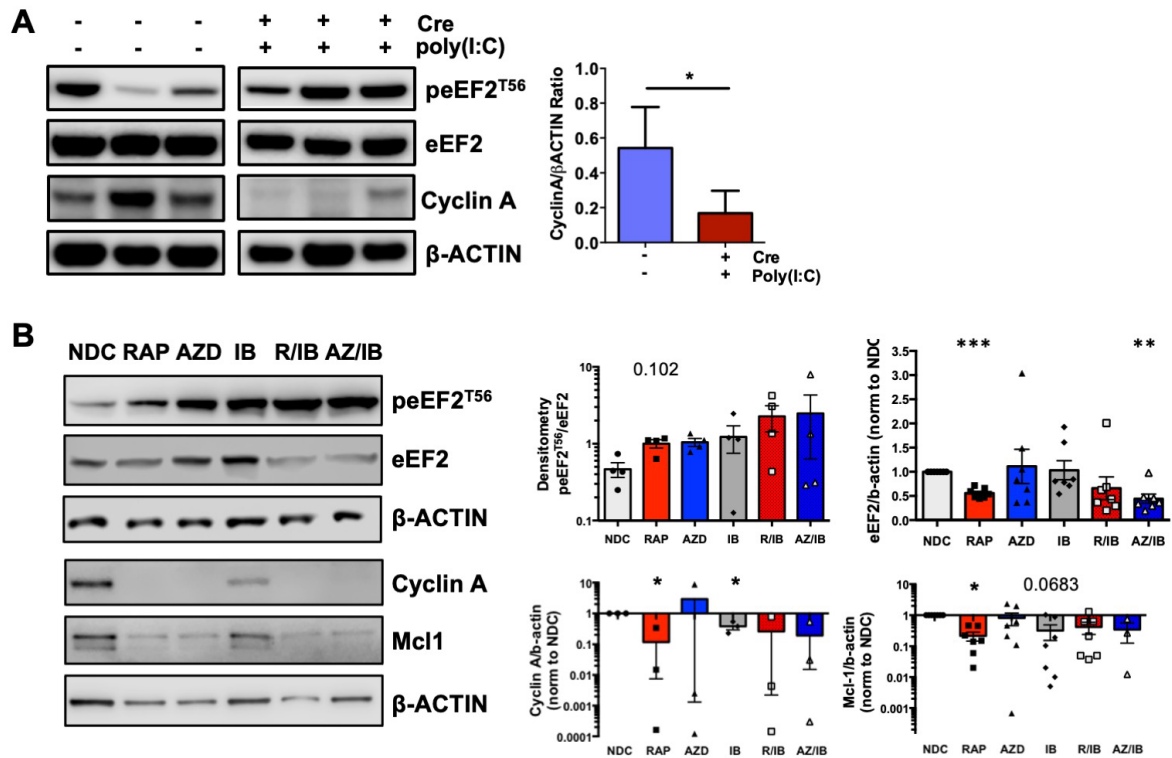
**Supplementary Figure 10: Gating strategy for PI staining in primary CLL cells.** Primary CLL cells were co-cultured for 5 days with CD40L expressing NTL cells with 15 ng/ml IL21 to induce proliferation in the presence of drugs, as indicated. The gating strategy used for the flow cytometry data to generate the average cell cycle phases summarised in Figure 6A is shown for one CLL patient sample. **A.** Cells were first gated by FSC vs SSC to determine the CLL population. Thereafter, only CLL cells within the cell cycle profile were gated (G0/G1 – G2), and the univariate modelling tool in FlowJo was used to generate the percentages of cell cycle analysis on these cells (G0/G1 phase, purple; S phase, yellow; G2 phase, green). **B.** FlowJo generated PI profiles for an individual patient sample (CLL147) treated with drugs as indicated.



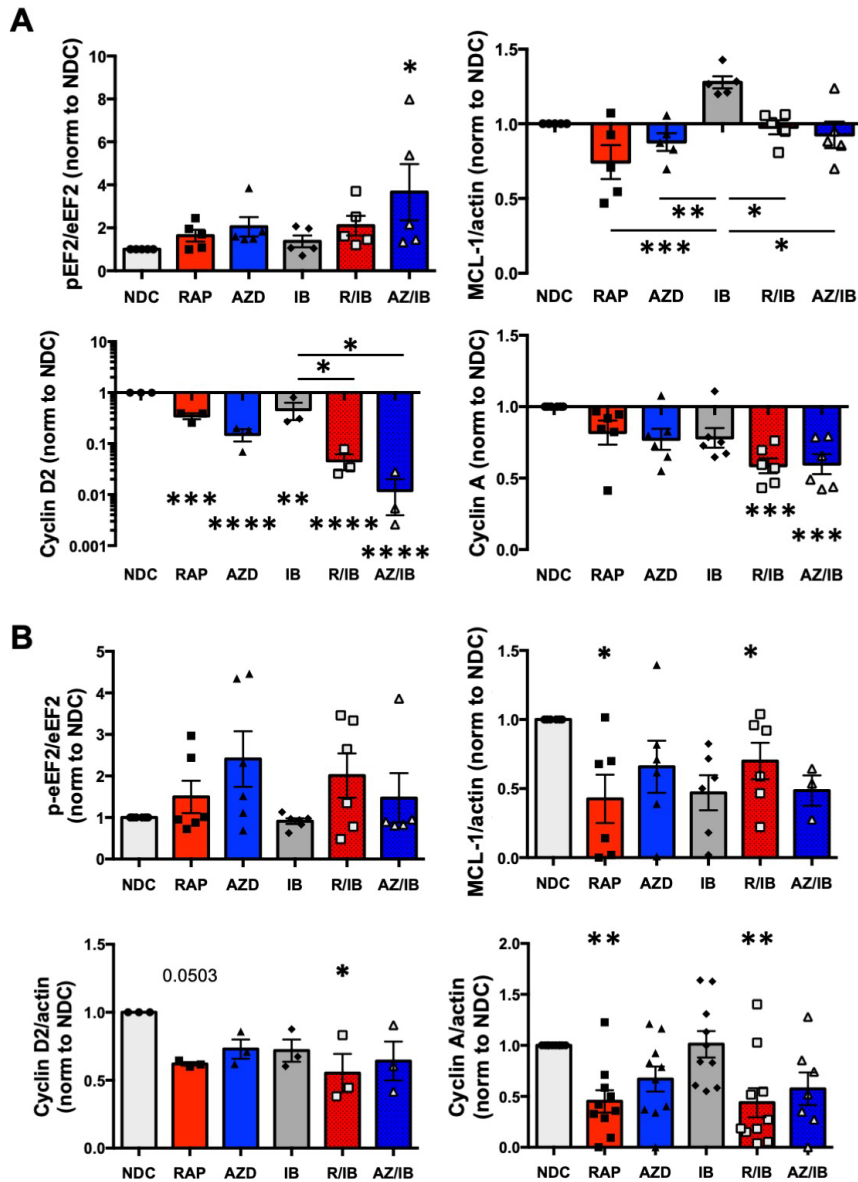
**Supplementary Figure 11: MEC1 cells exhibit decreased cell cycling, increased apoptosis and reduced proliferation with mTOR inhibitors and ibrutinib treatment.** Representative flow-cytometry plots (A) and graphs showing percentage of MEC1 cells in G0/G1 phase (B), S phase (C) and G2/M phase (D) when treated with vehicle control (NDC, light grey), rapamycin (RAP, red), AZD8055 (AZD, blue), ibrutinib (IB, dark grey) or RAP/IB (dark red). Representative flow-cytometry plots (E) and graphs demonstrating the percentage of live (F), early (G), and late apoptotic (H) MEC1 cells treated with NDC, RAP, AZD, IB or RAP/IB, as indicated. Representative CTV MFI (I) and graphs of CTV MFI ratios (J) of MEC1 cells assessed at 72 hr upon treatment with NDC, Rapa, AZD, Ibr or RAP/IB. Data are expressed as mean  $\pm$  SEM. p values were determined by an ordinary one-way ANOVA with Dunnett multiple comparisons test ( $p \leq 0.05$ ,  $p^{**} \leq 0.001$ ,  $p^{***} \leq 0.0001$ ,  $p^{****} \leq 0.00001$ ).



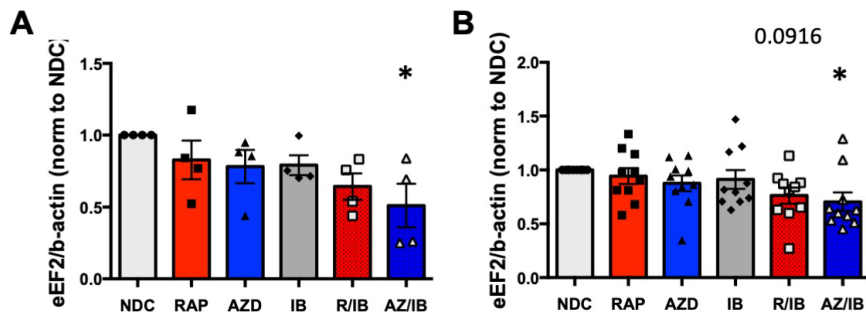
**Supplementary Figure 12: CLL primary cells exhibit altered eEF2 and eEF2k signalling with mTORC1 inhibition *in vitro*.** CLL cells were co-cultured for 5 days with CD40L producing NTL cells with 15 ng/ml IL21 to induce proliferation. Representative Western blot is shown in Figure 6I. Quantitative analysis of protein phosphorylation relative to loading control as indicated is shown: pAKT<sup>S473</sup>/AKT (**A**), p4EBP1<sup>T37/46</sup>/4EBP1 (**B**), pS6<sup>S235/236</sup>/β-Actin (**C**), peEF2K<sup>S366</sup>/β-Actin (**D**), pEF2<sup>T56</sup>/β-Actin (**E**) in primary CLL cells treated with rapamycin (RAP, red), AZD8055 (AZD, blue), ibrutinib (IB, dark grey), RAP/IB (dark red) or left untreated NDC, light grey). Blots shown are representative of at least 5 individual CLL patient samples. Data are expressed as mean ± SEM. p values were determined by an ordinary one-way ANOVA with Dunnett multiple comparisons test (p \* ≤ 0.05, p \*\* ≤ 0.001).



**Supplementary Figure 13: Raptor ablation after development of CLL-like disease *in vivo* inhibits Cyclin A and MCL1 expression.** **A.** NSG mice were transplanted with *Mx1-Raptor*-PKC $\alpha$ -KR cells to establish CLL-like disease. Protein lysates were prepared from spleen of these mice. Representative Western blot of indicated proteins in *Mx1-Raptor* control PKC $\alpha$ KR cells (n=3), or *Mx1-Raptor* cKO PKC $\alpha$ KR cells + poly(I:C) after disease development (n=3). These blots are the same as those shown in Figure 3J, therefore showing the same  $\beta$ -ACTIN loading control. Quantitative analysis of Cyclin A expression relative to loading control is shown. Data are expressed as mean  $\pm$  SEM (p  $\leq$  0.05). p values were determined by two-tailed unpaired *t*-test. **B.** PKC $\alpha$ -KR cells were co-cultured with OP9 cells to establish CLL-like disease *in vitro*. On d21 co-cultures were treated for 24 hr with rapamycin (RAP), AZD8055 (AZD), ibrutinib (IB), or a combination of RAP and IB (R/IB) or AZD and IB (AZ/IB) or NDC as indicated. Protein lysates were prepared and representative Western blots are shown (n $\geq$ 3 biological replicates). Densitometry plots of Western blots are shown, with graphs showing peEF2<sup>T56</sup>/eEF2 (n=4), eEF2/ $\beta$ -Actin (n=7) and Cyclin A/ $\beta$ -Actin (n=3) and Mcl1/ $\beta$ -Actin (n $\geq$ 3) relative to NDC. Data are expressed as mean  $\pm$  SEM, with p values were determined by an ordinary one-way ANOVA with Dunnett multiple comparisons test (p  $\leq$  0.05, p  $\leq$  0.001, p  $\leq$  0.0001).



**Supplementary Figure 14: mTOR inhibitors inhibit protein expression of protein associated with proliferation and MCL1 in human CLL cells.** MEC1 cells were treated with drugs for 24 hr (A) or proliferating CLL cells are co-cultured for 5-8 days with NTL-CD40L/IL21 in the presence of drugs (B) as indicated and the Western blots were carried out, representative of which are shown in Figure 7B&C. Quantitative analyses of protein phosphorylation/ expression relative to  $\beta$ -actin are shown: p-eEF2<sup>T56</sup>/eEF2, Cyclin A/ $\beta$ -Actin, Cyclin D2/ $\beta$ -Actin and Mcl-1/ $\beta$ -Actin in CLL cells treated with rapamycin (RAP, red), AZD8055 (AZD, blue), ibritinib (IB, dark grey), RAP/IB (dark red), AZ/IB (dark blue), or left untreated (NDC, light grey). Data are expressed as mean  $\pm$  SEM. p values were determined by an ordinary one-way ANOVA with Dunnett or Tukey multiple comparisons test ( $p \leq 0.05$ ,  $p^{**} \leq 0.001$ ,  $p^{***} \leq 0.0001$ ,  $p^{****} \leq 0.00001$ ).



**Supplementary Figure 15: Drug treatments reduce eEF2 protein expression in human CLL models.** MEC1 cells were treated with drugs for 24 hr (A), proliferating CLL cells are co-cultured for 5-8 days with NTL-CD40L/IL21 in the presence of drugs (B) as indicated. Western blots were carried out, representative of which are shown in Figure 7B&C. Quantitative analyses of protein phosphorylation/ expression relative to β-actin are shown: peEF2<sup>T56</sup>/eEF2, Cyclin A/β-Actin, Cyclin D2/β-Actin and Mcl-1/β-Actin in CLL cells treated with rapamycin (RAP, red), AZD8055 (AZD, blue), ibrutinib (IB, dark grey), RAP/IB (dark red), AZ/IB (dark blue), or left untreated (NDC, light grey). Data are expressed as mean ± SEM. p values were determined by an ordinary one-way ANOVA with Dunnett multiple comparisons test ( $p^* \leq 0.05$ ).